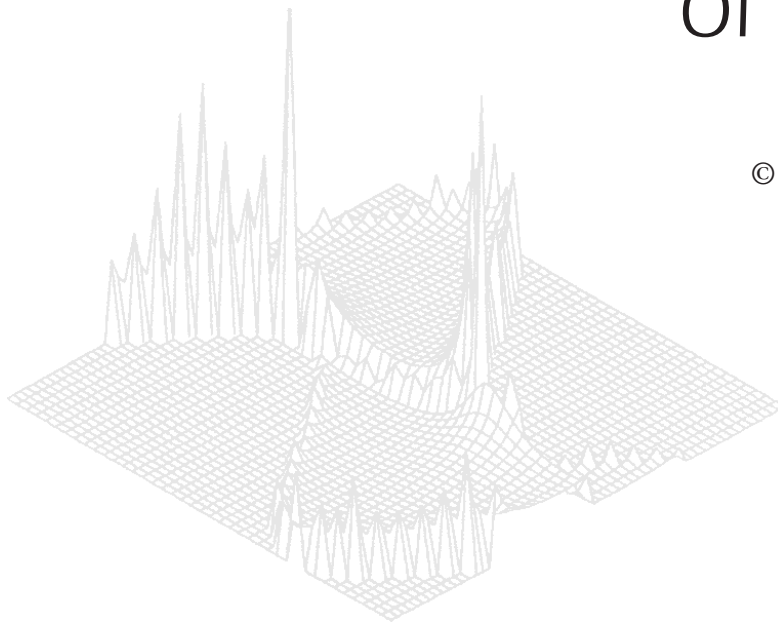

CSIRO PUBLISHING

Australian Journal of Physics

Volume 50, 1997
© CSIRO Australia 1997



A journal for the publication of
original research in all branches of physics

www.publish.csiro.au/journals/ajp

All enquiries and manuscripts should be directed to

Australian Journal of Physics

CSIRO PUBLISHING

PO Box 1139 (150 Oxford St)

Collingwood

Vic. 3066

Australia

Telephone: 61 3 9662 7626

Facsimile: 61 3 9662 7611

Email: peter.robertson@publish.csiro.au



Published by **CSIRO PUBLISHING**
for CSIRO Australia and
the Australian Academy of Science



Atomistic Simulation of Interfaces in Materials: Theory and Applications*

Irene Yarovsky

BHP Research Melbourne Laboratories,
245–73 Wellington Road, Mulgrave, Vic. 3170, Australia.

Abstract

The theoretical background, methodology and some applications of atomistic simulation of interfaces in materials are described in this paper. Interfaces between crystalline solids and polymers as well as between two polymers can be simulated using the methods described. Applications include various interfaces in a multilayered coated metal system. The methodology enables such properties as the work of adhesion, interfacial stability, degree of curing in polymers and permeability to small molecules to be predicted. In addition, interfacial structure and molecular mechanisms of adhesion and barrier performance of coatings can be revealed.

1. Introduction

Interfacial properties of materials are of prime importance to many industrial applications such as coatings, lubricants, adhesives etc. In particular, organic and inorganic coating materials are widely used for anticorrosion protection and aesthetic appearance of metallic products. An example of such a coated metal system is BHP's Colorbond® product. The Colorbond® material is a multilayered system comprising metal/inorganic, inorganic/organic and organic/organic interfaces. Properties and stability of each of these interfaces are crucial for short and long term performance of the product.

There is a constant search for new components of the Colorbond® coating system which will improve its chemical and physical properties. This process requires a better understanding of the structure/property relationship in materials currently used. Although some properties of current coating systems can be measured, an ability to predict properties of new coatings prior to the laboratory synthesis will significantly facilitate the new coating design. In addition, a fundamental understanding of coating performance mechanisms at the molecular level can significantly influence the design and development of coatings with improved properties.

Recent development of molecular simulation techniques provides a tool for predicting the interfacial structure and properties of organic coatings at the molecular level (Yarovsky and Chaffee 1995*a*, 1995*b*; Yarovsky 1995, 1996*a*, 1996*b*). In the present work, some of the techniques which have been applied

* Refereed paper based on a contribution to the ANZIP 20th Condensed Matter Physics Meeting held at Charles Sturt University, Wagga Wagga, NSW, in February 1996.

to study interfaces in the Colorbond® coating system are described. Most of the techniques are implemented in commercially available software developed and distributed by Molecular Simulations, Inc.

Details of the coatings systems studied and results obtained by means of the molecular simulations cannot be presented in the open literature due to commercial confidentiality of the research.

2. Theoretical Background

Many polymer surfaces and polymer/solid interfaces encountered in practice exhibit complex morphology or/and complex chemical characteristics. In particular, complex morphology may include partial crystallinity in the polymer, chain orientation induced by processing conditions, complicated surface topography of the solid, etc. Complex chemical characteristics may be related to polymer polydispersity, chemical and energetic heterogeneity of the solid surface, the presence of functional groups on the polymer or surface that can react chemically, or the presence of coupling agents (crosslinkers) or adhesion promoters. All or some of the above complexities are common for most interfaces in Colorbond®. In practice, only relatively simple systems, consisting of purely amorphous polymers formed by monodisperse, flexible, linear chains, and of molecularly smooth solid surfaces interacting with the polymers via London dispersion forces, may be simulated at the molecular level using current methodologies (Theodorou 1992). Modelling even such simple systems at the molecular level is quite challenging. For example, molecular weight distribution, i.e. the multiplicity of molecular chain lengths in polymer systems, ranging from that of an individual monomer unit (a few Å) to that of entire chains (on the order of 100 Å), is associated with a multiplicity of characteristic times for molecular motion, ranging from tenths of a ‘picosecond’ for bond vibrations to seconds for overall chain self-diffusion and conformational relaxation in high molecular weight melts. For the glass transition the relaxation times for long-range motion become too long to be modelled at the molecular level. Despite these difficulties, modelling approaches can be designed that offer a reasonable compromise between realism of molecular representation, fundamental rigour, and computational tractability in addressing the interface behaviour of pragmatically relevant amorphous polymer systems.

The conformation of flexible polymers in the amorphous bulk is essentially unperturbed by long-ranged interactions (Flory 1979) and can be characterised by the average radius of gyration and end-to-end distance. At an interface, special enthalpic and entropic factors cause the organisation of chains to deviate from their bulk characteristics and, in turn, govern all macroscopically manifested interfacial properties such as adhesion. Molecular dynamics (MD) based on direct, full atomistic calculation of the interfacial energy and the time development of an interface is the most accurate method for investigating the interfacial phenomena.

The following sections describe model building and simulation methodologies for different layers of coated metal systems: solid surfaces (metal oxides), amorphous polymers and their interfaces.

(2a) Atomistic Models of Crystal Surfaces

Crystalline materials have both translational periodicity and space group symmetry. The building blocks for description of a crystal structure include a

motif of *parent* atoms called the asymmetric unit, and a 3D reference system called a *lattice*. The lattice basis is usually referred to as the *unit cell*. For a full crystal structure definition a space group that comprises a set of symmetry operators should be specified. The symmetry operators and the unit cell translations act on a unique, asymmetric volume to generate the complete crystal structure. For a given crystalline material, the asymmetric unit is the smallest set of uniquely positioned atoms. All other atoms may be derived from these parent atoms. The crystal unit cell is usually described by the axial lengths, a , b and c , and the interaxial angles α (the angle between b and c), β (a and c) and γ (a and b). The space group symmetry that is present imposes constraints on the interaxial angles and on the relative axial lengths.

The construction of crystal models requires specification of the basis atoms, the unit cell, and the space group symmetry operators. The positions of the atoms of the asymmetric unit are usually given in crystallographic or fractional coordinates, that is, as fractions of the unit cell length, and are usually obtained from the literature or crystallographic databases. When an asymmetric unit and the symmetry information are specified, the crystal model, i.e. an extended structure model in which symmetry and translational periodicity information is retained, can be constructed. The spatial extent of the constructed model can be specified in a variety of ways to obtain the desired size, periodicity, and a crystal face of the model. In particular, 3D (crystal) or 2D (surface) structures may be constructed by choosing directions and/or constraints for periodic structure propagation. A particular surface Miller plane may be chosen as an alternative bounding definition. The size of the constructed crystal structure is usually defined according to the aim of modelling studies, as well as considering the computational power available.

A Miller plane (or a group of equivalent parallel planes) is a plane that contains interception points along the crystallographic a , b and c directions that are identical for every unit cell in the crystal structure. This definition requires that the interception points be integral fractions of the unit cell edge lengths. The integers called the Miller indices of the plane are labelled h , k and l . The most common surfaces of a crystal, i.e. those of low energy, are generally surfaces of low Miller index (Tasker 1984). These planes are closest packed with large interplanar spacing.

Alumina and chromia surfaces play an important role in the behaviour of the Colorbond® material. These metal oxide surfaces form interfaces with a primer coat (usually epoxy resin based paint). Adhesion and barrier properties of the interfaces are crucial for the product performance. The models of chromia and alumina surfaces are therefore being used to study the molecular mechanisms of adhesion at the metal oxide/primer interface of Colorbond®.

Models of alumina surfaces. Several structures have been reported for alumina (Al_2O_3), among which $\alpha\text{-Al}_2\text{O}_3$ is the most thermodynamically stable form. Alumina is obtained by thermal decomposition of aluminium hydroxide (Lippens and Steggerda 1970). The fundamental structure of $\alpha\text{-Al}_2\text{O}_3$ can be described as a hexagonally close-packed lattice of oxygen atoms with aluminium atoms distributed in octahedral interstices. The crystal structure was determined by Swanson and coworkers (Swanson *et al.* 1960) with space group $R\bar{3}c$ and unit cell parameters $a = b = 4.748 \text{ \AA}$, and $c = 12.991 \text{ \AA}$.

The (100) plane of an α -alumina crystal was assumed to be the predominantly exposed plane by Peri (1965) and Lippens (1961). However, the occurrence of various exposed crystal planes, which would have a different local environment, appears to be likely (Knozinger 1976).

Alumina surfaces previously exposed to water vapour (or moist air) at temperatures above 100°C are terminated by a monolayer of hydroxyl groups. The presence of hydroxyl groups in the surface has been shown by deuterium exchange and infrared spectroscopy (Peri and Hannan 1967; Peri 1965; Carter *et al.* 1965; Dunken and Fink 1966) and by chemical methods (Boehm 1966). Even after heat treatment *in vacuo* at 800°C, about 2% of the total hydroxyl content is still retained on the surface (Peri 1965). With heating, a water molecule is desorbed by combination of adjacent hydroxyl pairs leaving an oxide ion and an oxygen vacancy on the surface. Five kinds of hydroxyls have been identified according to the number of aluminium atoms bound to the hydroxyl and the coordination number of the aluminium atoms (Knozinger and Ratnasamy 1978). These different hydroxyl types are depicted in Fig. 1. Hydroxyls of type I are known to be basic, while hydroxyls of types II and III are acidic (Knozinger and Ratnasamy 1978). It was suggested (Peri 1965) that on the 100 plane each hydroxyl is equivalent. However, on other surfaces, it was shown that water molecules are usually removed by combination of a hydrogen atom from an acidic hydroxyl and a basic hydroxyl. Therefore, it seems likely that hydroxyls of type I are present on the 100 alumina surface, while hydroxyls of both types I and II are present at the 001 alumina surface (Yoshida 1990).

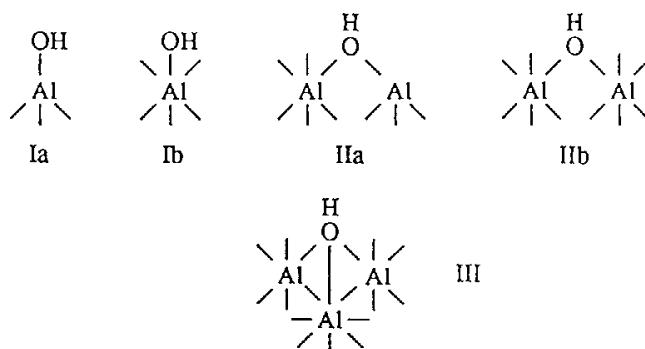


Fig. 1. Different types of hydroxyl groups present on an alumina surface.

Four models of alumina surfaces were constructed on the basis of the above considerations obtained from the literature. Two models represented the aluminium oxide surfaces 100 and 001, and two further models represented the alumina hydroxide surfaces 100 and 001. The models of oxide surfaces were constructed first according to the unit cell and space group symmetry information as described in Section 2a. The alumina models were then modified to obtain the hydroxide surfaces.

In the modelling studies discussed in this work the surface model coordinates obtained by the above procedures were kept fixed in subsequent Molecular Dynamics simulations.

Models of chromia surfaces. The crystal structure of α -Cr₂O₃ is made up by a hexagonal close-packed lattice of oxide ions similar to that of α -Al₂O₃. Two thirds of the octahedral sites are occupied by Cr³⁺ ions. The unit cell is characterised by $a = b = 4.9589 \text{ \AA}$, $c = 13.59308 \text{ \AA}$, as well as the symmetry constraints for hexagonal crystal structure. The 001 face is the most likely crystal plane to predominate in the external surface of well crystallised α -Cr₂O₃ (Zecchina *et al.* 1971). For this reason, the 001 face (predominant for chromia) was chosen for comparison with the 100 face (predominant for alumina) for both chromia and alumina surface models.

A model for the dehydroxylated 001 face was proposed by Zecchina and coworkers (Zecchina *et al.* 1971). Equal numbers of four- and five-coordinated Cr³⁺ ions are distributed on this idealised surface. It was shown by Zecchina *et al.* (1971) that complete hydroxylation of α -Cr₂O₃ does not occur. Assuming random removal of hydroxyl groups from a hydroxylated α -Cr₂O₃ surface, similar to that proposed by Peri (1965) for α -Al₂O₃, one would expect the generation of coordinatively unsaturated Cr³⁺ ions and O²⁻ ions of widely differing local configurations, resulting in a heterogeneous surface (Knozinger 1976). However, because of the lack of experimental information on precise atomic details of the surface structure, molecular modelling studies were focused on 'neater' situations, i.e. fully dehydroxylated (oxide) surfaces and hydroxylated (hydroxide) surfaces of α -Cr₂O₃ and α -Al₂O₃. The Cr₂O₃ surface models were constructed analogously to those of Al₂O₃.

(2b) Atomistic Models of Amorphous Polymers

Setting up the initial configuration of an amorphous polymeric system requires some special considerations in addition to those required when modelling atomic or small-molecule liquids or solids. In the latter case, it is generally sufficient to begin with any regular crystal lattice where the lattice spacing is chosen to obtain the desired density of the system. Then molecular dynamics simulation is started with random atomic velocities chosen from a Maxwellian distribution for a given temperature, resulting in the fairly rapid conversion of the structure to equilibrium (Allen and Tildesley 1987). In the case of polymers, it is important to start with a configuration in which backbone conformer population and the global characteristics of the chains (e.g. mean-squared radius of gyration) are representative of the most probable states of the material being studied.

A method first employed by Theodorou and Suter (1986) involves creation of an initial guess structure, followed by relaxation of the structure to a state of minimum potential energy. The periodic system is formed from a single molecule subjected to a simple cubic repeating scheme as illustrated in Fig. 2. Each cell may therefore be considered to comprise a portion, or portions, of a parent chain, plus a series of image chains which are merely displacements of the parent molecule along the x , y and z directions by some integer multiple of the cell edge length.

The Theodorou–Suter chain generation approach attempts to satisfy the requirements that the initial configuration be 'typical' of one which would be found with significant probability. This approach is based on the widely accepted idea that the configurational statistics of a chain in the bulk is well represented by an independent rotational isomeric state (RIS) model which can be used as a basis for generating chains in a bulk system (Flory 1989).

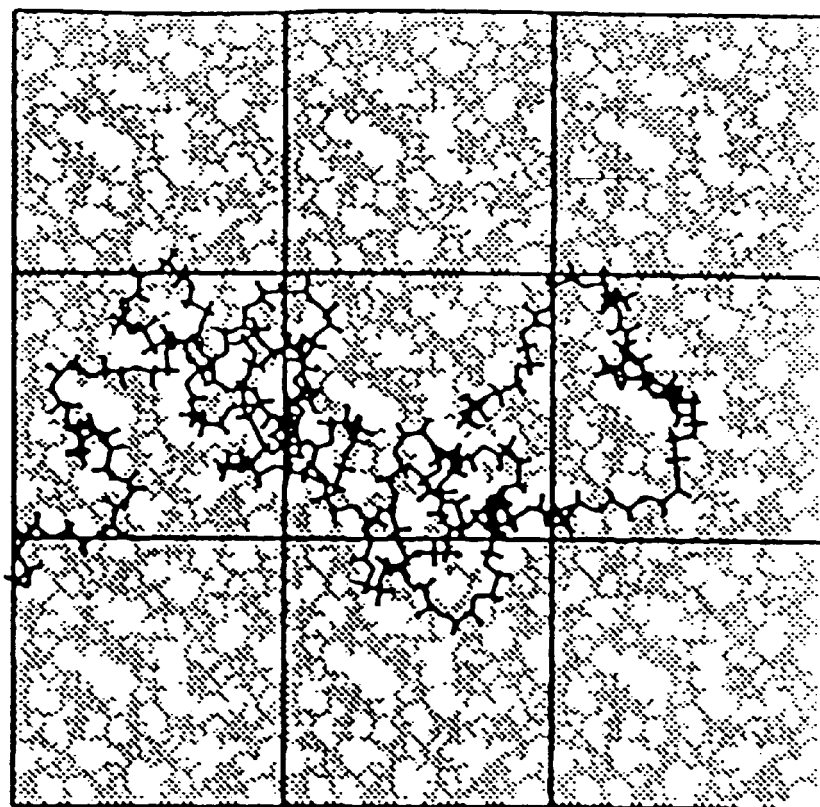
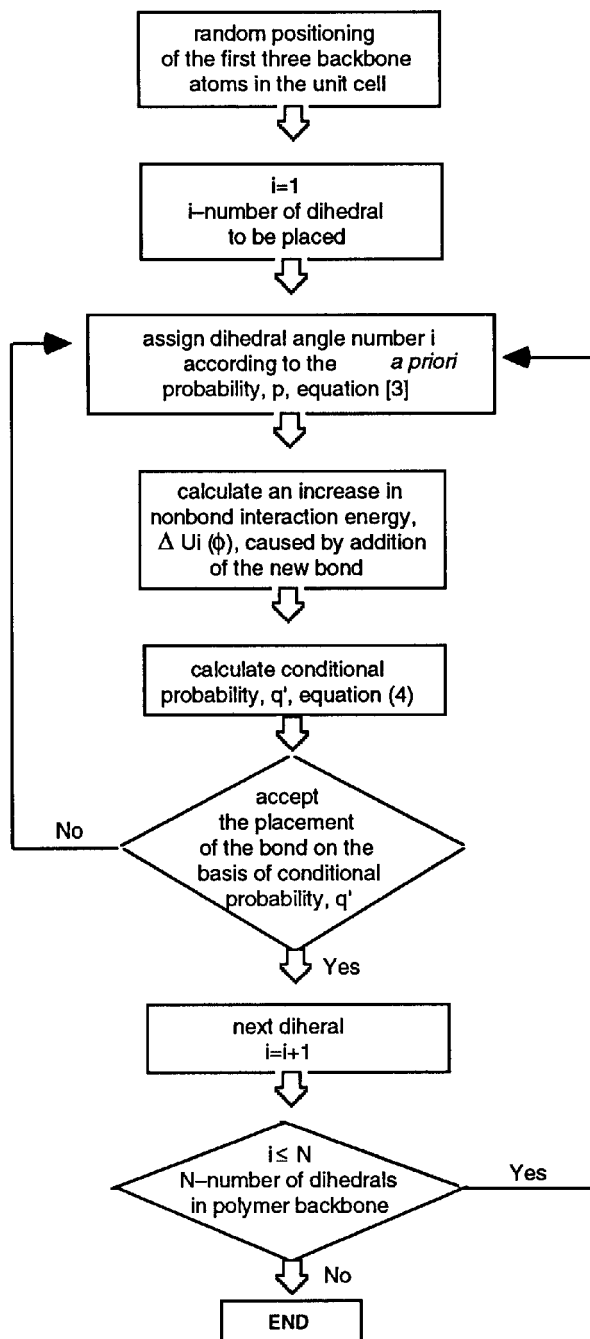


Fig. 2. Two-dimensional projection of a single parent molecule (highlighted) within a system with periodic boundaries.

The RIS approach takes advantage of the fact that in determining the overall configuration of a linear (i.e. unbranched) chain, the most important degrees of freedom are torsional rotations about the bonds of the backbone. The force constants for other degrees of freedom, such as bond bending and stretching, are so large that bond angles and lengths do not vary greatly from their equilibrium values. Consequently, such motions generally make little contribution to the gross conformation of a chain. In the RIS scheme, all degrees of freedom except torsions in the backbone are explicitly neglected. However, the effect of these neglected degrees of freedom is implicitly taken into account in determining the statistical weights of particular conformations.

A torsional angle may, in principle, adopt a continuum of values from -180° to $+180^\circ$. For the purpose of determining configurational statistics, the RIS approximation treats a torsional angle in a chain's backbone as if it can adopt only a discrete subset of these values. The justification for this is made clear by inspecting a plot of the potential energy as a function of the dihedral angle. Such a plot obtained by performing a conformational analysis typically contains a small number of distinct minima, separated by relatively high energy barriers. Thus, a typical RIS model considers only the discrete values for any given torsional angle, corresponding to the minima in the energy profile. Although only a single

SCHEME 2



where $\Delta U_i(\phi)$ denotes the increase in nonbonded interaction energy caused by addition to the system of skeletal atom $i+1$ plus pendant atoms of skeletal atom i . The factor $q_{i-1,i}(\phi', \phi)$ denotes the conditional probability of finding bond i in state ϕ when bond $i-1$ is known to be in state ϕ' . In turn, q may be defined in terms of bond and bond-pair *a priori* probabilities p , obtained using RIS theory (equation 3) by the relationship

$$q_{i-1,i}(\phi', \phi) = p_{i-1,i}(\phi', \phi)/p_{i-1}(\phi'). \quad (5)$$

The state of bond i is then chosen in accordance with the modified conditional probabilities q' .

The initial guess generation described above should be followed by an energy minimisation in which all bond lengths and valence angles are held fixed and the backbone rotation angles and Euler angles describing the overall orientation are used as degrees of freedom. Molecular dynamics can also be used as a highly effective structure refinement tool. Scheme 2 illustrates the above Theodorou–Suter procedure for constructing an amorphous polymer.

(2c) Models of Interfaces

To ensure the further ability to build up two-layered polymer systems from the separate layers, the unit cells with identical a and b dimensions should be constructed. In order to achieve the correct density of the resultant systems the third, c , dimension (i.e. layer thickness) is calculated using the following relationship:

$$c_2 = c_1(m_2/m_1)(d_1/d_2), \quad (6)$$

where c_2 and c_1 , m_2 and m_1 , d_2 and d_1 are respectively thickness, mass and density of the two cells to be layered (Polymer User Guide 1996). Construction of 2D periodic systems differs from the bulk (3D) system construction in two important respects. First, the construction effectively places hard walls on two opposite cell faces (in xz plane—see Fig. 3). Chain construction must then ensure that no bond crosses these hard walls. Second, an energy penalty proportional to the inverse ninth power of the distance of an atom i from the wall is added to the total energy of the system. Therefore, in the 2D cells there is some strain imposed by these additional forces. This strain is removed by relaxing the systems in 3D space as described in Section 3. The 2D cells are only used for construction of two-layered systems.

To improve the reliability of the modelling it is important to average simulated properties over many configurations. This is a consequence of statistical mechanics that any fluctuation involving an energy penalty of less than kT is likely to contribute significantly to macroscopic properties. Thus, a distribution of values is expected for any property. Therefore, an ensemble of several configurations is constructed for each polymer in the manner described above. Examples of the 2D cells generated are presented in Fig. 3. The vacuum spacers arising from the application of 2D periodicity can be seen at the top and bottom of the generated cells.

In order to eliminate a vacuum layer between the two polymer layers originating from the building procedure, molecular dynamics is performed with 3D periodic boundary conditions. This procedure results in formation of interfaces where alternating polymer layers are in immediate van der Waals contact with each

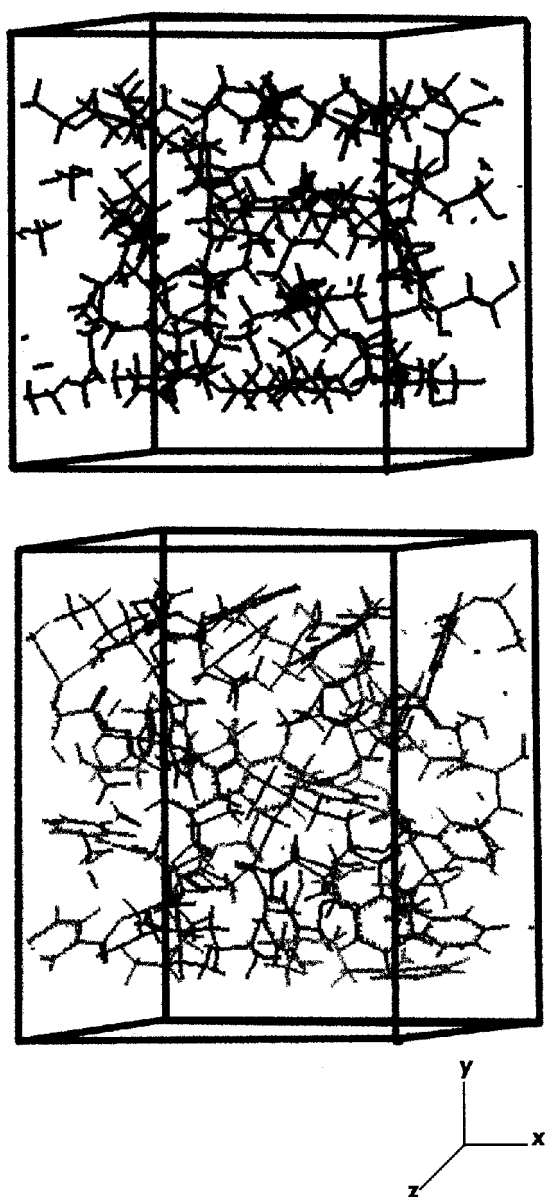


Fig. 3. Illustration of the simulated 2D polymer layers for building an interface. Unit cells only are shown. Vacuum spacers on the top and bottom of both cells are clearly visible.

other (Fig. 4). The tension as well as non-uniformity at the bottom, middle and top of the cell arising from employing 2D periodicity were thus removed by relaxing the system in three dimensions as fully described in the next section. The resultant systems contain two identical primer/top coat interfaces (due to the 3D periodicity) which are infinite in the x and z directions and edge effects are eliminated.

In order to predict environmental stability of the interfaces, dry and wet systems can be simulated. In particular, in order to simulate the wet interfaces, the systems are solvated with water filling all the available free volume. This represents the extreme case which may take an indefinite time to occur in reality. However, the value of the work of adhesion in the extreme case will allow the long term interfacial stability to be predicted. In addition, the molecular mechanism of adhesive bond displacement by water can be revealed and the diffusion constant for water can be calculated. Therefore, both dry and wet systems can be simulated for each type of constructed interface.

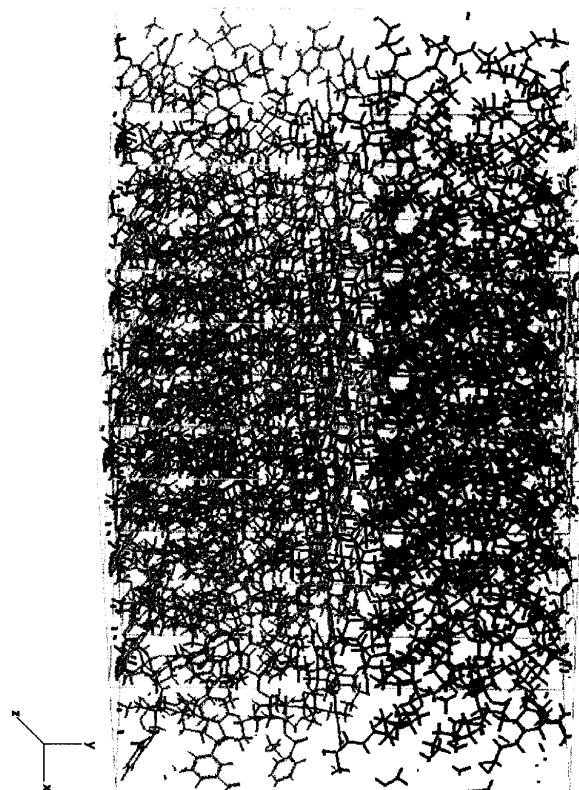


Fig. 4. Illustration of a typical polymer/polymer interface obtained by the atomistic simulation. A 2D periodic system is shown. Some degree of interpenetration of the two polymer layers can be seen.

A model of the solid/polymer interface can be built analogously to the polymer/polymer interface simply using the 2D periodic solid surface model (as emerged from the building procedure described in Section 2*a*) in place of one of the polymer layers.

(2d) Molecular Dynamics

The molecular dynamics (MD) method is employed for simulation of the interfaces between the model systems described in Sections 2*a* and 2*b*. In this method a trajectory of the molecular system is generated by simultaneous integration of Newton's equation of motion for all the atoms in the system:

$$d^2\mathbf{r}_i(t)/dt^2 = m_i^{-1} \mathbf{F}_i, \quad (7)$$

where \mathbf{r}_i are atomic coordinates, t is time, m_i are atomic masses, and \mathbf{F}_i is the force on atom i which is calculated as

$$\mathbf{F}_i = -\partial E(\mathbf{r}_i \cdots, \mathbf{r}_N)/\partial \mathbf{r}_i, \quad (8)$$

where $E(\mathbf{r})$ is the potential energy function.

The potential energy function typically includes bond length stretching and bond angle bending terms, torsion twisting term, out-of-plane deformation term for planar systems, as well as Lennard-Jones and Coulombic terms describing the non-bond van der Waals and electrostatic interactions:

$$E = E_b + E_a + E_t + E_p + E_{\text{vdW}} + E_{\text{el}}. \quad (9)$$

The functional form of the energy expression is determined by a forcefield, a typical example being the CVFF forcefield (Dauber-Osguthorpe *et al.* 1988):

$$E_b = \sum D_b [1 - e^{-\alpha(b-b_0)}]^2, \quad (10)$$

$$E_a = \sum H_\theta (\theta - \theta_0)^2, \quad (11)$$

$$E_t = \sum H_\phi [1 + \cos(n\phi)], \quad (12)$$

$$E_p = \sum H_\chi \chi^2, \quad (13)$$

$$E_{\text{vdW}} = \sum \sum (A_{ij}/r_{ij}^{12} - B_{ij}/r_{ij}^6), \quad (14)$$

$$E_{\text{el}} = \sum \sum q_i q_j / \epsilon r_{ij}, \quad (15)$$

where b, θ, ϕ represent internal coordinates, i.e. bond length, bond angle and torsion angle respectively, with their unstrained standard values denoted by the subscript 0: χ is the current value of the out-of-plane torsion angle (for example in a benzene ring); r_{ij} is the interatomic distance for atoms i and j ; q_i and q_j are the partial charges carried by each atom; and ϵ is the dielectric constant. The parameters $D_b, H_\theta, H_\phi, H_\chi$ are the force constants for the corresponding intramolecular deformations. Further, A_{ij} and B_{ij} are the parameters for the non-bond repulsive and dispersive interactions. There is no special term for hydrogen bonding in the CVFF forcefield as van der Waals and electrostatic parameters of this forcefield have been shown to be sufficient for the fit of CVFF to experimental data on hydrogen bonding (Hagler *et al.* 1979a, 1979b). An extended form of the original CVFF forcefield, the CVFF_CALP forcefield, is parametrised for organic/inorganic interactions.

Typical interfacial structures obtained by the MD procedure are shown in Figs 4 and 5.

3. Interfacial Properties

The main objective of the MD studies was to design approaches that may be useful for predicting microscopic structural, thermodynamic and short-time

dynamic properties of the idealised interfaces. These approaches are described in this section.

(3a) Structure of the Interface

The microscopic structural features of a polymer/polymer interface include the overall spatial distribution, shape, and orientation of chains, as well as a degree of interpenetration of chains, and can be derived from the radial distribution functions constructed for different polymer groups. The radial distribution function

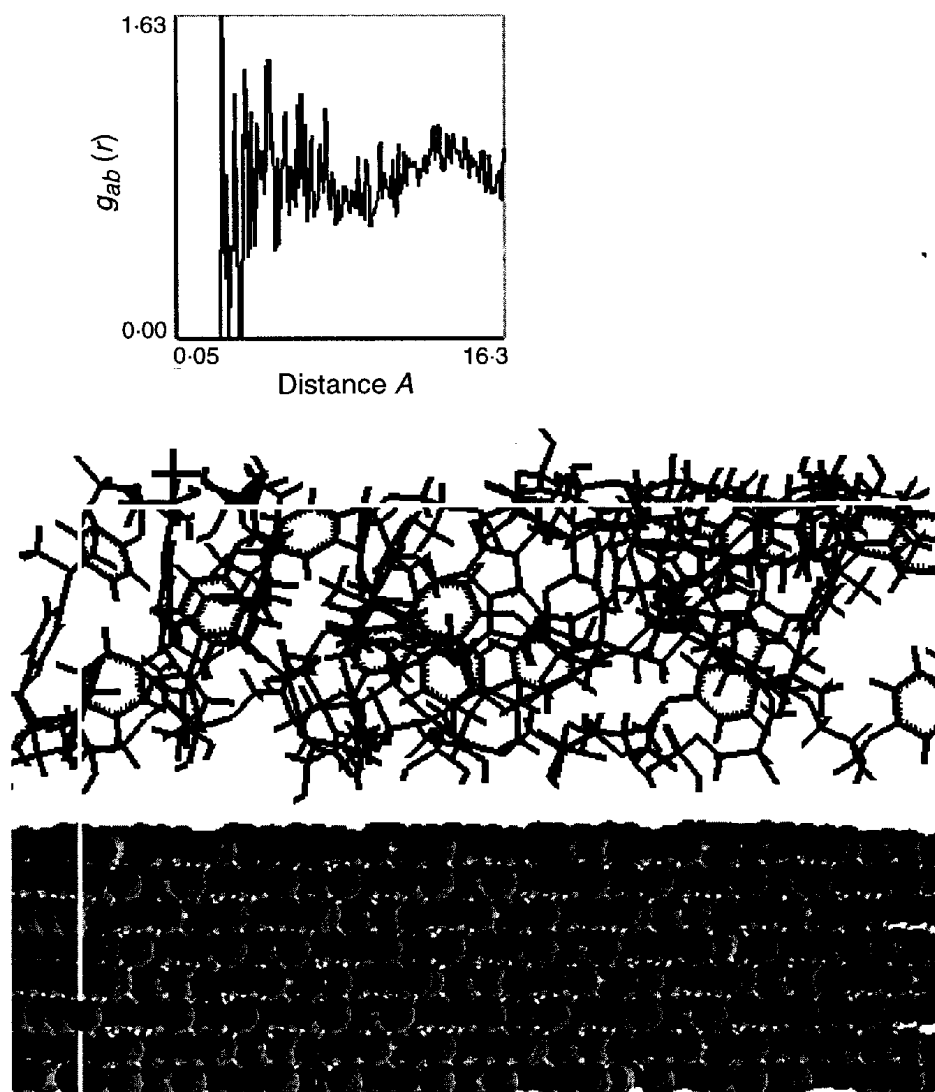


Fig. 5. Illustration of a typical metal oxide/polymer interface obtained by the atomistic simulation. Chemical groups of the polymer coordinated towards the metal oxide surface (mostly hydroxyl groups) are responsible for adhesion. An example radial distribution function for the polymer hydroxyl groups and top oxygen atoms of the surface is also shown. The first peak indicates hydrogen bonding present at the interface.

(RDF) gives a measure of the probability that, given the presence of an atom at the origin of an arbitrary reference frame, there will be an atom with its centre located in a spherical shell of infinitesimal thickness at a distance r from the reference atom (Allen and Tildesley 1987). This concept also embraces the idea that the atom at the origin and the atom at distance r may be of different chemical types α and β . The resulting function is then commonly given the symbol $g_{\alpha\beta}(r)$. It is also referred to as the pair correlation function. The total pair correlation function $g(r)$ is defined as the probability of finding any two atoms at a distance r apart in the simulated structure relative to the expected probability calculated for a completely homogeneous phase with random atoms (Allen and Tildesley 1987). In the simulated structure, $g(r)$ can be calculated using the expression (Theodorou and Suter 1986):

$$g(r) = \frac{\rho_r}{\rho} = \frac{N_r V}{N(4\pi r^2)dr}, \quad (16)$$

where ρ_r is the number of atoms in the volume element, ρ is the overall density, N_r is the number of atoms inside the shell, N is the total number of atoms in the system, and V is the defined volume. Using the RDFs it is also possible to determine the existence and degree of specific interactions like hydrogen bonding or hydrophobic association. An example RDF for hydroxyl groups in the polymer and oxygen atoms in the top surface layer is shown in Fig. 5. The hydrogen bonding between the layers of the system is clearly indicated by the sharp first peak in the RDF at $\sim 2.7 \text{ \AA}$.

(3b) Interfacial Adhesion

Interfacial thermodynamic properties, in particular the work of adhesion in the case of polymer/polymer interfaces, can also be determined from the MD simulations. The work of adhesion W_a is a measure of attraction of two solids A and B, and can be described as the work required to separate a solid phase AB into two surfaces A and B (VanKrevelen 1990). This quantity is given by the relationship of Dupre (1869):

$$W_a = \gamma_A + \gamma_B - \gamma_{AB}, \quad (17)$$

where γ_A and γ_B is the specific surface free energy of phase A and B (surface tension), and γ_{AB} is the specific interfacial free energy of contacting phases A and B (interfacial tension).

In the presence of a wetting liquid (denoted by the suffix 'L'), the work of adhesion W_{aL} is

$$W_{aL} = \gamma_{AL} + \gamma_{BL} - \gamma_{AB}. \quad (18)$$

It is known (Kinloch 1979; Gledhill and Kinloch 1974) that for a typical organic adhesive/metal oxide interface W_a in an inert atmosphere, i.e. dry air, usually has a large positive value, indicating thermodynamic stability of the interface. However, in the presence of a liquid, W_{aL} may have a negative value, indicating the interface is now unstable and will dissociate (Table 1). Thus, calculation of the terms W_a and W_{aL} may enable the environmental stability of an interface to be predicted.

Table 1. Values of W_a and W_{aL} for various interfaces obtained by contact angle measurements

Interface	Work of adhesion (mJ m^{-2})	
	Inert medium W_a	In water W_{aL}
Epoxy/ferric oxide	291	-255
Epoxy/silica	178	-57
Epoxy/aluminium oxide	232	-137

The specific surface and interfacial energies can be calculated directly from MD simulations of bulk amorphous polymers and a composite system consisting of alternating layers of each polymer or solid and polymer layers. Although trends in the work of adhesion obtained from the simulation are well reproduced experimentally (in ‘stronger or weaker adhesion’ terms for various systems) (Yarovsky and Chaffee 1995*a*, 1995*b*), absolute values of the calculated work of adhesion cannot be expected to be the same as experimentally measured values for several reasons. First of all, simulated adhesion values represent ‘fundamental’ adhesion, i.e. adhesion due to forces between materials while in experiments ‘practical’ adhesion is measured which depends strongly on experimental set up, conditions, operator skills etc. There is no adhesion test yet which would measure ‘fundamental’ adhesion between materials to enable quantitative comparison of simulation results with experiments. Another reason is that simulated work adhesion values depend on the forcefield used in the simulation, i.e. the mathematical form of equations describing forces between materials, for example equations (9)–(15) used in this work. Quality of the forcefield is one of the most important issues in molecular simulations and it is being constantly improved via validation work performed by the software developing companies and other research groups. At the same time, it should be noted that trends in adhesion rather than absolute values represent the most valuable information for materials design since the known trends allow research and development work to be narrowed and be properly focused on required materials properties.

An alternative way of calculating surface and interfacial free energy is based on experimental values of contact angles measured for different liquids on surfaces forming an interface (Owen and Wendt 1969; Kaelble and Uy 1970; Kaelble 1970). This technique can be used in order to obtain another estimate of interfacial stability as well as to validate molecular modelling results. Some examples of values of W_a and W_{aL} obtained by the above technique are shown in Table 1 (Kinloch *et al.* 1975; Butt and Cotter 1976).

The change from a positive to negative work of adhesion provides a driving force for the displacement of adhesive on the substrate surface by water. It is therefore expected that if a joint is subjected to a humid environment there will be a progressive encroachment into the joint of the bonded interface. This will have the effect of progressively reducing the joint strength.

This thermodynamic approach may be employed to predict the stability of *any* interface in *any* liquid, provided chemisorption and interdiffusion across the interface are absent. It should be noted, however, that the thermodynamics give no information on the expected service life of joints in hostile environments as the rate of interface debonding is controlled by the availability of water at the interface governed by diffusion of water through the adhesive. The diffusion rate

is in turn a complex function of many chemical and physical parameters such as the polymer chemical composition (particularly hydrophilicity), molecular weight, temperature etc. However, the dynamics of an interface can also be estimated from molecular simulations for model conditions, as described in the next section.

(3c) Barrier Properties of the Interface

The barrier properties of organic coatings, i.e. the transport of penetrant molecules (in particular those of water and oxygen) through the coatings is crucial for anticorrosion protection of an underlying metal substrate. The permeability is the most important quantifier of the transport of penetrant molecules through polymers. The barrier performance of a polymer can be defined as its resistance to the transport of penetrant molecules, i.e. as the inverse of its permeability.

The permeation of small molecules through polymers usually occurs by the solution-diffusion mechanism which has two key steps (Bicerano 1993). The penetrant molecule is first sorbed by the polymer, i.e. dissolves in the polymer structure. Then the permeability is controlled by the diffusion of the small molecule through the polymer. The permeability is therefore equal to the product of the diffusivity (diffusion coefficient) and solubility. Although it is not yet possible to predict solubility using the atomistic simulation techniques, the diffusion constants for small molecules in a polymer matrix can be calculated from long term MD. The absolute values of the calculated diffusion constants should not, however, be considered for direct comparison with experimental values due to several assumptions used in the idealised models of coatings and limited simulation time. At the same time, the predicted values can be used for a relative comparison of different (possibly theoretical) materials and the trends obtained may be used for direction of future polymer design.

The time dependence of the average mean squared displacements (MSD) of the centre of mass of the polymer chains (or small molecules, i.e. solvent or gas) over all chains (small molecules) in the simulation and multiple time origins t_0 can be calculated according to the following relationship:

$$\text{MSD} = \sum_{i=1}^N \langle [\mathbf{R}_i(0) - \mathbf{R}_i(t)]^2 \rangle, \quad (19)$$

where \mathbf{R}_i is the position of the particle centre of mass, N is the number of particles of a given type, and the angle brackets denote averaging over all choices of time origin. This quantity is calculated directly from the MD trajectory over a long time period (usually more than 1 ns).

To estimate the relative mobility of the simulated molecules, diffusion coefficients D for the molecule centre of mass are calculated. Diffusion coefficients can be obtained from the MSD of the centres of mass using the Einstein relation (Allen and Tildesley 1987) as follows:

$$D = \frac{1}{6N} \lim_{t \rightarrow \infty} \frac{d}{dt} \sum_{i=1}^N \langle [\mathbf{R}_i(0) - \mathbf{R}_i(t)]^2 \rangle. \quad (20)$$

Therefore, diffusion coefficients are calculated directly from the slope of the MSD versus time curves obtained from the MD simulation for a relatively long time (several hundred picoseconds depending on the size of the molecules in a system).

Several factors play a key role in determining the relative diffusivity of different penetrant molecules permeating a polymer by the solution-diffusion mechanism. First of all, it is the free volume available for the penetrant molecule to traverse the polymer. It should be noted that in contrast to the total free volume in the polymer matrix, the free volume available for diffusion is a function of the molecular size of a penetrant. Secondly, the cohesive forces between the polymer chains affecting the chain mobility are also crucial since there exists a correlation between the chain mobility (rigidity) and diffusion constants of penetrant molecules (Choi and Jo 1995). Finally, the diffusivity (and solubility) can be affected very significantly by the strength of the interactions between the penetrant molecule and the structural units in the polymer chains, especially by the specific interactions such as hydrogen bonding and hydrophobic clustering. All these effects can be revealed from the atomistic simulation of polymer systems in addition to the relative values of diffusion constants.

4. Conclusions

The techniques and methodologies described in this work were used to investigate the fundamentals of adhesion at various interfaces of the Colorbond® coating system. Molecular mechanisms of the adhesion formation and failure were revealed that helped to direct further research and synthesis work for the coating components with improved properties. In addition, such properties as a degree of curing in polymers and coatings permeability to water and oxygen were predicted. Possible effects of these properties on adhesion and anticorrosion protection of steel are now being investigated.

At the same time, there are still serious limitations in molecular level coatings research. In particular, only simplified polymer models can yet be investigated, i.e. not including pigments, binders and other solid components. Ideal surfaces of the metal oxides should, in principle, be substituted by more realistic mixed oxide amorphous surfaces. Unfortunately, surface structures with experimental detail sufficient to enable a realistic molecular model to be built are not yet available. Most importantly, the studies described in this work focus only on the physical type of interactions in the coating systems (van der Waals and electrostatic), while in reality there exist mixed physico-chemical interactions including covalent bonding between the components of the coating systems. However, recent developments in computational chemistry methods are very promising in terms of delivering methodologies for modelling physico-chemical interactions in large molecular systems.

Overall, computational chemistry is increasingly becoming an advantageous aid for the design of materials, not only for advanced university centres but also for actual industrial manufacturers.

References

- Allen, M. P., and Tildesley, D. J. (1987). 'Computer Simulation of Liquids' (Clarendon: Oxford).
- Bicerano, J. (1993). 'Prediction of Polymer Properties' (Marcel Dekker: New York).
- Boehm, H. P. (1966). *Adv. Catal. Relat. Subj.* **16**, 179.
- Butt, R. I., and Cotter, J. L. (1976). *J. Adhesion* **8**, 11.
- Carter, J. L., Lucchesi, P. J., Corneil, P., Yates, D. J. C., and Sinfelt, J. H. (1965). *J. Phys. Chem.* **69**, 3070.

- Choi, K., and Jo, W. H. (1995). *Macromolecules* **28**, 8598.
- Dauber-Osguthorpe, P., Roberts, V. A., Osguthorpe, D. J., Wolff, J., Genest, M., and Hagler, A. T. (1988). *Proteins* **4**, 31.
- Dunken, H., and Fink, P. (1966). *Z. Chem.* **6**, 194.
- Dupre, A. (1869). 'Theorie Mechanique de la Chaleur' (Paris).
- Flory, P. J. (1979). 'Principles of Polymer Chemistry' (Cornell University: Ithaca).
- Flory, P. J. (1989). 'Statistical Mechanics of Chain Molecules' (Interscience: New York).
- Gledhill, R. A., and Kinloch, A. J. (1974). *J. Adhesion* **6**, 315.
- Hagler, A. T., Lifson, A., and Dauber, P. (1979a). *J. Am. Chem. Soc.* **101**, 5122.
- Hagler, A. T., Lifson, A., and Dauber, P. (1979b). *J. Am. Chem. Soc.* **101**, 5131.
- Kaelble, D. H. (1970). *J. Adhesion* **2**, 66.
- Kaelble, D. H., and Uy, K. C. (1970). *J. Adhesion* **2**, 50.
- Kinloch, A. J. (1979). In 'Adhesion', Vol. 3 (Ed. K. W. Allen) (Applied Science Publishers: London).
- Kinloch, A. J., Gledhill, R. A., and Dukes, W. A. (1975). In 'Adhesion Science and Technology' (Ed. L. H. Lee), p. 597 (Plenum: New York).
- Knozinger, H. (1976). *Advances in Catalysis* **25**, 184.
- Knozinger, H., and Ratnasamy, P. (1978). *Catalysis Rev.* **17**, 31.
- Lippens, B. C. (1961). Ph.D. Thesis, Delft University of Technology.
- Lippens, B. C., and Steggerda, J. J. (1970). In 'Physical and Chemical Aspects of Adsorbents and Catalysts' (Ed. B. G. Linsen), p. 171 (Academic: London).
- Owen, D. K., and Wendt, R. C. (1969). *J. Appl. Polym. Sci.* **13**, 740.
- Peri, J. B. (1965). *J. Phys. Chem.* **69**, 220.
- Peri, J. B., and Hannan, R. B. (1967). *J. Phys. Chem.* **71**, 695.
- Polymer User Guide (1996). Molecular Simulations, Inc.
- Swanson, H. E., Cook, M. I., Isaaks, T., and Evans, E. H. (1960). National Bureau of Standards, Circ. No. 539, **9**, 3.
- Tasker, P. W. (1984). In 'Advances in Ceramics', Vol 10 (Ed. W. D. Kingery), pp. 176–89 (Am. Ceramic Soc.: Columbus, OH).
- Theodorou, D. N. (1992). In 'Physics of Polymer Surfaces and Interfaces', Ch. 7 (Butterworth-Heinemann, Stoneham, MA).
- Theodorou, D. N., and Suter, U. W. (1986). *Macromolecules* **19**, 139.
- VanKrevelen, D. W. (1990). 'Properties of Polymers' (Elsevier: Amsterdam).
- Yarovsky, I. (1995). Molecular modelling investigation of Corstrip® adhesion to Colorbond®, BHPR TechNote No. BHPR/CP/N/004.
- Yarovsky, I. (1996a). Atomistic simulation of the primer/top coat interface in Colorbond®, BHPR Report No. BHPR/CP/R/010.
- Yarovsky, I. (1996b). New theoretical method for prediction of structure and properties of crosslinked polymers. Application to Cr-free epoxy primers, BHPR TechNote No. BHPR/SC/N/008.
- Yarovsky, I., and Chaffee, A. L. (1995a). Adhesion at the interface between Zinalume® and primer: A molecular modelling investigation, BHPR Report No. BHPR/CP/R/005.
- Yarovsky, I., and Chaffee, A. L. (1995b). Effect of primer chemical composition and molecular weight on adhesion to Zinalume®, BHPR Report No. BHPR/CP/R/018.
- Yoshida, S. (1990). In 'Theoretical Aspects of Heterogeneous Catalysis' (Ed. J. B. Moffat), p. 506 (Van Nostrand Reinhold: New York).
- Zecchina, A., Coluccia, S., Guglielminotti, E., and Ghiotti, G. (1971). *J. Phys. Chem.* **75**, 2774.